

# Kidney Tumour Detection Using Deep Neural Network

Tawseeful Haziq<sup>1</sup>, Ashish Obroi<sup>2</sup>, and Yogesh<sup>3</sup>

<sup>1</sup>M. Tech Scholar, Department of Computer Science & Engineering, RIMT University, Mandi Gobindgarh, Punjab, India

<sup>2</sup>Head, Department of Computer Science & Engineering, RIMT University, Mandi Gobindgarh, Punjab, India

<sup>3</sup>Associate Professor, Department of Computer Science & Engineering, RIMT University, Mandi Gobindgarh, Punjab, India

Correspondence should be addressed to Tawseeful Haziq; [showkat.tahir@gmail.com](mailto:showkat.tahir@gmail.com)

Copyright © 2022 Made Tawseeful Haziq et al. This is an open access article distributed under the Creative Commons Attribution License, which permits unrestricted use, distribution, and reproduction in any medium, provided the original work is properly cited.

**ABSTRACT-** Classifying the malignancy of a renal tumour is one of the most important urological duties because it plays a key role in determining whether or not to undergo kidney removal surgery (nephrectomy). Currently, the radiological diagnostic made us 89++ing computed tomography (CT) scans determines the likelihood of a tumour being malignant. However, it's believed that up to 16 percent of nephrectomies may have been avoided since a postoperative histological study revealed that a tumour that had been first identified as malignant was actually benign. Numerous false-positive diagnoses lead to unnecessary nephrectomies, which increase the chance of post-procedural problems. In this article, we offer a computer-aided diagnostic method that analyses a CT scan to determine the tumour's malignancy. The prediction, which is used to identify false-positive diagnoses, is carried out following radiological diagnosis. Our solution can complete this challenge with an F1 score of 0.84. Additionally, we suggest a cutting-edge method for knowledge transmission in the medical field using colorization-based pre-processing, which can raise the F1-score by as much as to 1.8.

**KEYWORDS-** Deep neural, Renal tumour, CT-Scan, Benign, Malignant

## I. INTRODUCTION

With an estimated incidence of more than 73,000 new cases in America in 2020 and its number rising every year, renal cancer is a dangerous illness (Cokkinides 2020). Currently, the radiographic diagnosis of the tumour is the main factor in determining whether to undergo kidney removal surgery (nephrectomy) or segmentectomy (operation to remove portion of a kidney or tumour). Most of the time, the choice comes down to determining the tumour's malignancy or benignity based on factors like its density and the sort of attenuation shown on CT scans, among others. However, despite having been identified as malignant during radiological diagnosis, 13 percent to 16 percent of excised tumour may really be benign (Kay and Pedrosa 2018). The inability to effectively calculate the benefit-risk ratio between doing a nephrectomy or segmentectomy and leaving the tumour under surveillance is a result of the rise in false-positive malignancy predictions. Malignant tumours raise the danger of more operations and may potentially result in the patient's death. However, if the tumour is benign, it is frequently safer to

forego the procedure and leave it alone. This is particularly true for senior people since being older reduces the possibility that the tumour may grow over time and raises the danger of the procedure. According to a research, radical nephrectomy was strongly linked to mortality from any cause in individuals over the age of 65 [7]. Since those people make up the majority of instances of kidney tumours, there is an urgent need to reduce the number of false-positive malignant tumor diagnoses.

This study shows the effectiveness of a deep learning-based approach may be used to reduce the number of false-positive predictions, with the model's purpose being to act as a second opinion system used in addition to the radiological diagnostic. Given its high specificity, such a model should serve as a catalyst to alert physicians to cases that could be incorrectly categorized as malignant and, as a result, reduce the number of false-positive occurrences. Its function is to comfort physicians about their diagnosis or alert them to a potential error. Figure 1 displays the system's suggested implementation. The diagnosis can then be confirmed or refuted by other testing, such as a biopsy, or by consulting with other specialists. Although considered the gold standard for classifying kidney tumours, biopsies come with added risks and expenses [6] In the research, we demonstrate a deep learning model that has been trained to differentiate between benign and malignant tumours using a CT scan. The model can provide results with an accuracy of 86% and a strong recall. We compare the effectiveness of well-known pre-trained neural networks in the job of predicting the aggressiveness of tumours. In addition, we demonstrate how picture colorization enhances knowledge transfer across the pretraining and fine-tuning stages, increasing accuracy in the medical image classification job.

## II. LITERATURE REVIEW

In a research by Liu et al. [2], they employed CT colonography photos for 141 exophytic systemic lupus erythematosus, 38 isolates renal lesions, and 71 standard cases absent malignant tumors in order to detect exophytic tubular tumours using machine learning approaches. The right and left kidneys were both segmented as part of the prep, which was carried out using the belief propagation strategy for background subtraction. This method reduced the search region of renal abnormalities. Relating a feature selection method to the results of manifold diffusion and looking for invaginations brought on by the lesion allowed

the features to be retrieved. The suggested model achieved great effectiveness with rates of susceptibility of exophytic injury and endophytic hole identification of 95% and 80%, etc, relying based their research observations.

Deep learning techniques were used in a study by Attia et al. [3] to classify kidneys in ultrasound imaging. The abnormal eye cases comprised renal failure, kidney damage, angiomyolipoma, organ tumours, and cystic renal disease. They employed 66 ultrasound images of normal and abnormal kidneys from the Ultra scan Centre in India. The Principle Component Analysis (PCA) was used to simplify the problem of the produced features, which were based on multi-scale wavelets that were retrieved from the scans' Region of Interest (ROI). The suggested model was built using a neural network with two convolution layer and one hidden nodes for multi-class classifying, and it achieved a 97 percent accuracy rate for classifying the five examples correctly.

### III. METHODOLOGY

#### A. Kidney Disease (KD)

The human body absorbs the nutrients it needs from meals, returning the wastes to the blood, where they may harm the body if they remain. Due to the approximately one million small filters called nephrons that operate to process the flowing blood, the kidneys play a significant role in filtering these waste items from the blood [7]. The kidneys also produce vitamin D, prevent heart disease, and stimulate the creation of red blood cells in addition to regulating saline and chemical volumes. Through tubes known as ureters, the kidneys discharge urine into the bladder, which is then emptied through the urethra [8]. We may conclude that kidneys are crucial to maintaining a person's life. Back discomfort beneath the ribs and pain around the kidneys are two symptoms of renal disease, as are fever, nausea, and increased urination. Blood, urine, ultrasound, and imaging tests can all be used to identify kidney pain. Hypertension, which together account for up to 70% of KD cases [9], are two distinct causes of KDs. High blood sugar levels can lead to diabetes, which damages the body's organs, including the kidneys [10]. When blood artery walls are subjected to elevated blood pressure, hypertension results [11]. When blood pressure is not under control, renal disease may result and vice versa.

#### B. Kidney Tumours (KT)

A benign or malignant renal function tumour is the formation of glandular growth in one or both kidneys [5]. Kidney cells are impacted by the illness KT. According to doctors, Kidney Tumours start when "mutations" or changes" take place" in the DNA of specific kidney cells, where the DNA gives instructions for the cell to test that it should expand and divide swiftly. Additionally, the tumour may originate from inside the nephron, and in rare cases, it is a secondary tumour that had already reached epidemic proportions from nearby organs, such as a lesion [7]. Cells may develop and spread to other parts of the body. Different individuals are affected variously by KT, which results in various sensations and indicators including a

reduction in libido or an unusual loss of weight, which impacts their daily activities [8]. About 3.7 fraction of all malignancies in the US are kidney tumours. Kidney cancer affects more than 62,000 Americans each year. With age, kidney cancer becomes more common. It is more likely to affect males than women [9]. Figure 1 depicts an example of both healthy and tumor-free organs.

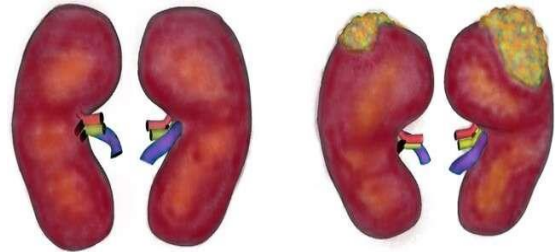


Figure 1: Illustration comparing tumour-free and tumour-ridden kidneys

#### C. Factors Affecting Tumour Formation

Medical professionals are still unsure about the causes of KT. Although the specifics of a renal cell case are unconfirmed, there are some factors that are expected to raise the risk of KT, including smoking, irradiation, being male (men are about twice as likely as women to build a KT), drinking alcohol and coffee, eating foods high in fat and chicken, and eating healthy. Therefore, the excess weight may result in hormonal changes that raise the risk. A personal history of KT, exposure to compounds like hydrocarbons, acetone, or agrochemicals, and sick people with lymphoma are at an increased risk of developing KT for unknown reasons. Chemical drugs, such as long-term use of specific painkillers like Parasytose or Revanin, may also lead to alterations in the genetic makeup. These health conditions do not make you more likely to acquire a KT, but they certainly increase your risk [9].

In a study on the factors associated for nephron tumours, Gago et al. [10] analysed data from 550 people with RCC to demonstrate that family history is a possible risk factor. These patients ranged in age from 25 to 74. Additionally, thorough information gathered through a quiz and in-person interviews on personal history of injury, kidney stones, medical history, medicines, and other lifestyle variables demonstrated the presence of a link. A second-degree relative with a kidney disease was also associated with an increasing risk of getting kidney tumours, and having a first-degree family with a liver tumour greatly increased the risk of kidney cancer by 95%. Smoking, persistent obesity, high blood pressure, having previously undergone an operation.

#### D. Kidney Tumour Types

KT is a collection of diverse genetic traits, genomics features, and, to some extent, clinical symptoms that develop from various locations of the nephron and include both aggressive (cancerous) and neutral (noncancerous) tumour [3]. Types of kidney tumours are depicted in Figure 2.

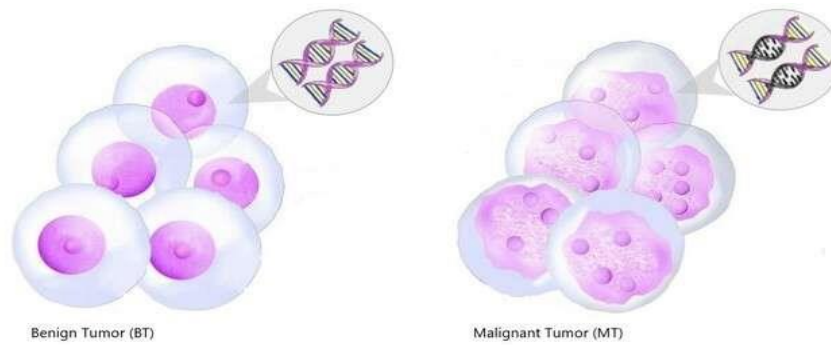


Figure 2: Examples of several kidney tumour kinds

The development of a benign tumour (BT) of the kidney is constrained. It also doesn't invade neighbouring tissues or propagate to other bodily cells [3]. Additionally, they are often treated with surgery and do not come back. There are many different kinds of non-cancerous malignancies [3], and most of the time they pose a minimal hazard to survival since they can develop into cancer if left untreated.

After the carcinoma was surgically removed, Anthony T. Corcoran et al. started researching on the tumour's diagnostic type, including whether it appeared benign or malignant [4]. The researchers obtained data from PubMed and oncology conventions. There were 26 studies gathered, which had images of 27,272 patients. As renal cells that tumour size was analyzed, the association between tumour size and hazardous features was also investigated, and a statistically significant correlation across cancer and cancer was discovered. According to the findings, 15 percent of surgically excised renal masses were benign tumours, and 85 percent were cancerous tumours.

The cancerous growth known as a malignant tumour (MT) begins in the kidney it spreads. By separating from a melanoma and moving via the lymphatic or circulation, cells in malignancy tumours can infect endothelium and create new tumour in other parts of the body. Tumour (supplementary tumour), which is the spread of cells from one organ to some other, is one of the main reasons why people die from cancer [5]. Cancers are initially physically removed, then radiation is used to eliminate any leftover cancerous cells, or chemotherapeutic is used alone if the tumor is too tough to try and remove in its last stages.

#### E. Kidney Tumour Stage

The pace of remission from the diseases may depend on the state of the growth, thus it is important to identify the grade of the lesion in order to choose the best treatment plan and the right way for taking medication in light of the situation. Figure 3 depicts the phases of a kidney neoplasm.



Figure 3: Stage of pancreatic tumour illustrated

A medical investigation concerning tumour staging was carried out by Reznik et al. [7]. There is a definite correlation between tumour size and the spread of metastases, according to data using CT and MRI scans. Stage scope of tumour dispersion and survival also have a direct association with one another. This is why it has recently been established that venous invasion shortens survival time and that tumours are a reliable sign of poor treatment outcomes.

Staging is crucial when thinking about a divisional myomectomy since research shows that substantial laparoscopic procedure greatly increases survival rates and now has subsequently been the norm for treated RCC. The

investigation involved getting a bottom-up scan with a 5 mm interferometer and finding, characterizing, and sequencing the tumours. Positive outcomes have been obtained using CT and MRI, response options of up to 30% have been recorded, and patient close is advised following surgical excision.

#### F. Radiology Imaging

Radiology imaging is the ou alors application of technology to learn about the interior makeup of human body organs. It helps patients live better lives by enabling more accurate and speedy diagnosis, as well as fewer side effects and effective complete treatment. Radiology

imaging is the primary method for finding tumours [8]. Unfortunately, there aren't any reliable clinical markers for diagnosis; as a result, therapeutic success depends on precise diagnosis and early discovery. Typically, [9] is how medical staff finds KT;

- Computed Tomography (CT): commonly used to determine the degree of RCC in the renal regions. CT scans can disclose information about just the hospital's tumour's placement, thickness, and growth to all other organ, as well as aid distinguish solid sizes from cyst ones. A prior research found that the effective differences between some of these types may be utilized to detect RCC in adults using tomographic Scanning characteristics [1].
- Angiography (CTA): This radiograph treatment aids in the diagnosis of cancer by providing a means of examining blood vessels in the eyes. In this disease diagnosis, the patient is given comparison, and the direct comparison dye helps to show incorrectly oriented blood arteries that are assumed to be connected to the tumour [3,8]. An summary of the applications, benefits, and drawbacks of radiation is provided in Table 1 below. Deployment of a System

### G. Dataset

We collected 15485 CT images coming from 383 individual cases. These data came from two sources. 173 of the cases were collected by us, using historical data of the patients that had undergone the nephrectomy. Every single case, in addition to CT images, was paired with histopathological results from the postoperative biopsy -

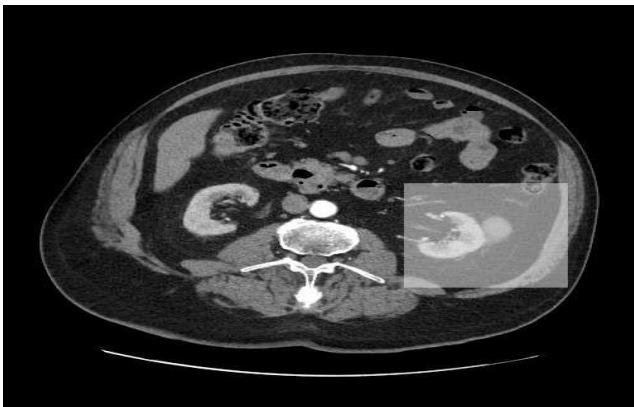


Figure 4: Visualization of the area cropped from full abdominal CT image

Detailed dataset description, distinguishing histopathological subtypes has been provided in the Table 1.

Next, we grouped the histopathological subtypes together into malignant and benign binary classes - ccRcc, chRcc and pRcc tumours were marked as malignant, and oncocytoma, angiomyolipoma (AML) and benign-other tumours were marked as benign.

As the KiTS19 dataset contained only the arterial phase of the study, we decided to use the very same phase during training and classification. This was also motivated by the fact that the arterial phase shows attenuation of tumours and, therefore, is suitable for malignancy prediction.

Table 1: Dataset with respect to different phases

Tumour type	No. of cases	No. of images
ccRCC	214	10193
chRCC	26	1590
pRCC-type-1	10	488
pRCC-type-2	3	324
pRCC	27	769
malignant-other	1	75
oncocytoma	20	702
AML	78	1221
benign-other	4	123
malignant tumours	281	13439
benign tumours	102	2046
total	383	15485

In our baseline experiments, we use a single 2D slice per case where the visible tumor area is the largest (as such images are the best reference for the case). We test the effect of using all the available 2D slices per case, utilizing the full dataset.

### H. Pre-Processing

The images themselves were firstly processed in DICOM format, where image data is presented as a 2D array of Hounsfield units (HU). Those units, ranging from -1024 to 3071, represent the attenuation coefficient measurement (with respect to water and air) during a CT scan 1.

$$HU = 1000 \times \frac{\mu_x - \mu_{water}}{\mu_{water} - \mu_{air}} \quad (1)$$

In line with the current standard for viewing abdominal CT scans, we cropped this range with a window center of 60 HU and window width of 400 HU. After cropping the values, we scaled them to represent grayscale pixel values ranging from 0 to 255. The images were also resized to 256x256 pixels to fit the size of popular pre-trained architectures.

### I. Colorization

Currently, ImageNet is the most popular dataset for pretraining large convolutional models. Results show that despite the significant differences in modality, models pretrained on ImageNet can still achieve better results in medical image classification than models trained solely for this task. However, medical images such as CT, MRI or X-ray are processed in grayscale format and must be converted to a 3-channel format in order to be processed by a pretrained network. The most common technique for doing this is to copy the grayscale values across different channels. This can, however, lead to a sub-optimal utilization of filters learned from colour images in transfer learning (Xie and Richmond 2018). In our solution, we

tackled this problem by pre-processing the images using colorization models. Those models deal with image-to-image prediction problems by reconstructing the image in RGB colour space based on its grayscale equivalent. Most of the popular models are based on pre-trained image classification models that are later adopted to the colorization task by conversion to fully convolutional networks.

In the initial experiments, we tested 3 popular open source image colorization models. The first model, Let there be Colour (LTBC) [8] uses an end-to-end network that jointly learns global and local features of an image. This is done through utilization of 2 convolutional networks — one for detection of global features and the other for detection of local features. These network outputs are then concatenated and used by the decoder network to produce colorized versions of the image. The second model, described in Learning Representations for Automatic Colorization (LRAC) (Larsson, Maire, and Shakhnarovich 2016), uses architecture based on a deep convolutional network — VGG16. It takes spatially localized multi-layer slices as per-pixel description, predicting chroma distribution of pixels given its hypercolumn descriptor. The third model — Colorful Image Colorization (CIC) [11] uses a VGG-styled network with added depth and dilated convolutions to map a grayscale image to its colored version. It is also noteworthy that this version of the network contains no pooling layers, and texture adjustments are made by spatially upsampling or upsampling multilayer blocks.

Results of colorization of an abdominal CT scan using different methods are shown in Figure 5. Having tested different solutions through visual examination of how well they improve the contrast of anatomical structures, we decided to use the Colorful Image Colorization framework. The authors claim that their model produces colorization that is more vibrant and perceptually realistic than the other approaches. This can be particularly useful in our case, as seen in the Figure 3. Other image colorization models produce results that are much less vibrant and, therefore, there is no clear semantic separation between different organs. Figure 4 shows Visualization of the area cropped from full abdominal CT image kidney (orange), bones (white) and other organs (red), while Figure 3 shows a separation between the tumor (red) and the rest of the kidney. This is likely due to the fact that authors show that their solution is suitable not only for colorization but also for semantic segmentation task what we show is also true for the medical domain. In the section, we show that this improves the classification performance.

Pre-trained networks. In our initial experiments, we tested architectures using popular pre-trained convolutional networks, including VGG16 [10] networks that replace filters with huge kernels and numerous follow 3-dimensional filters, Xception [7] based on pointwise convolution followed by (red) and the rest of the kidney. A depthwise convolution, ResNet [5] based on deep residual connections and DenseNet [6] based on connecting each layer to every other layer in a feed-forward fashion.

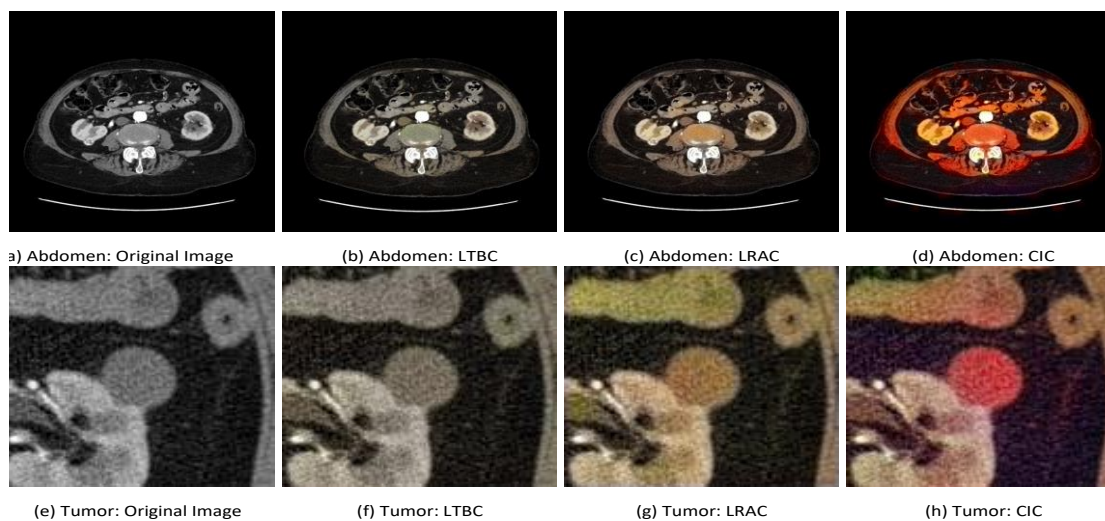


Figure 5: Comparison of different colorization models

Comparison of different colorization models: Learning representation for automatic colorization and colorful image colorization. Models based on (b) and (f) and (c, g) show little color difference between various parts of the CT Scan while the results based on Colorful image Colorization (d) show clear distinction between bone kidney (orange) and the rest of the organs (red)

All those models were pre-trained on ImageNet before the fine-tuning task of tumor malignancy prediction. Additionally, we also employed the DenseNet-based CheXNet system [9] that was built on NIH dataset containing 112 120 frontal-view X-ray images that has also

been proven to achieve accuracy in medical image analysis higher than models pre-trained on natural images.

In all cases, the model's classification layers were replaced by a custom unified classifier described in the following section.

Classification layers. In each case, the base networks were followed by the global average pooling layer with dropout of 0.2 and batch normalization. Next, the inputs were fed to two dense layers with 2048 neurons each and ReLU activation function. Those layers were also regularized with L2 type regularization. Subsequently, we applied another dropout of 0.2. The dropouts were crucial in the

architectures in order to prevent the overfitting of the network with the class imbalance in the dataset. Ultimately, after the two hidden layers, there was a final classification layer with SoftMax activation function to map the inputs into tumor malignancy. The visualization of the architecture is shown in Figure 4.

We used a binary cross-entropy loss function as each image should be mapped to exactly one tumor type. For the optimization, we used Adam algorithm[3] ). To deal with the class imbalance problem, the disproportionate amount of malignant tumors in the dataset, we applied class weight of 0.1 to the malignant cases. This has prevented the network from over-fitting and additional bias towards malignant tumors Dataset

Motivated by the limited size of our dataset, to test our solution we constructed a 5-fold cross-validation set stratified by the tumor malignancy. Cases were chosen from the historical data of patients that underwent nephrectomy based on the radiological diagnosis of the tumor being malignant. Each of the cases was paired with the postoperative histopathological results (considered a gold standard in renal tumor prediction) dictating whether the tumor was, as previously assumed, malignant, or in fact benign.

#### J. Pre-Trained Networks

In the initial experiments, we tested the performance of popular pre-trained architectures described in the previous section. In each case, the hyper-parameters of the networks were identical as outlined in the part before. Table 2 displays the evaluation's findings. The results show that the

best pre-trained network turned out to be DenseNet, achieving the F1-score of 80%. Another noteworthy fact is that CheXNet achieved the lowest score of all tests of pretrained encoders indicating that knowledge transfer from chest X-ray images was not beneficial over ImageNet, despite the fact that X-ray images and CT scans might be considered more similar than CT scans and natural images from ImageNet.

Table 2: Comparison of the pre-trained models.

Architecture	F1-score
CheXNet	0.7233
ResNetV2	0.769
Xception	0.7772
VGG16	0.8011
DenseNet	0.8046

#### K. Colorization

Based on the experiments described in the previous subsection, we chose DenseNet-based network as the baseline for further experiments. Comparing its performance with and without the colorization pre-processing (described in section 3), we can see in Table 3 that colorization improves the F1 score by 1.8 percent

Table 3: Effect of image colorization

Model	F1-score
DenseNet (without colorization)	0.8046
DenseNet (with colorization)	0.8228

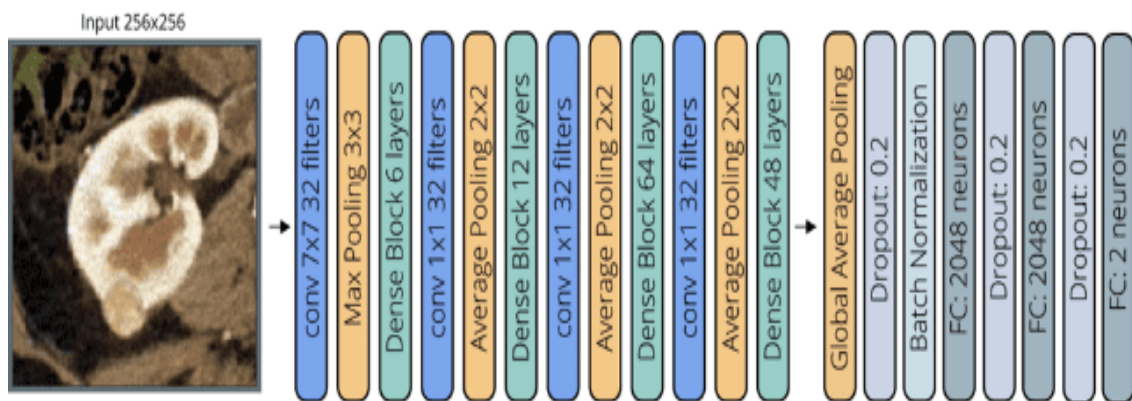


Figure 6: Architecture of the network

DenseNet encoder is followed by a classification block consisting of global average pooling, 2 hidden layers and the classification layer mapping the output to binary/malignancy prediction

#### L. Adding Additional Slices Per Tumor

Additionally, we also tested the effect of using additional 2D slices per single case in the training phase. This can be seen as an augmentation method where instead of providing the network with one reference image per case we use multiple CT slices per case depicting the tumor from different depths. This increased our dataset size from 383 images to 15485 images. To test the effect of adding additional slices, in the testing phase we used a single

image per case where the tumor is best visible, similarly to previous subsections.

Table 4: The effect of adding additional CT slices per case

Model	F1-score
DenseNet (with colorization, single slice)	0.8228
DenseNet (with colorization, all slices)	0.8444

In Table 4, we can see that providing the networks with additional CT slices increases its F1-score by up to 2.2 pp.

**M. Final Solution**

For the final solution, based on the results obtained in sections above, we chose the pre-trained DenseNet network fine-tuned on the colorized CT images from the full dataset. This network is able to achieve 0.84 F1-score, 0.86 accuracy, 0.79 precision and 0.86 recall. The high recall is especially important as it depicts the model’s ability to recognize cases misclassified in the initial radiological diagnosis.

**IV. SIMULATION AND RESULTS**

The CNN model was evaluated on the test set and the results are reported in Table 5. The detection performance of CNN cancer detection model achieved an accuracy of 84 percent and loss of 0.4.

This section shows the results obtained over the epochs 1, 5 and 10. The accuracy and other features kept on improving as we kept on increasing the no. of epochs in the systems. The following figures from figure 7 to figure 9 show the confusion matrices when the epochs were 1, 10 and 20 respectively.

*Epoch=1*

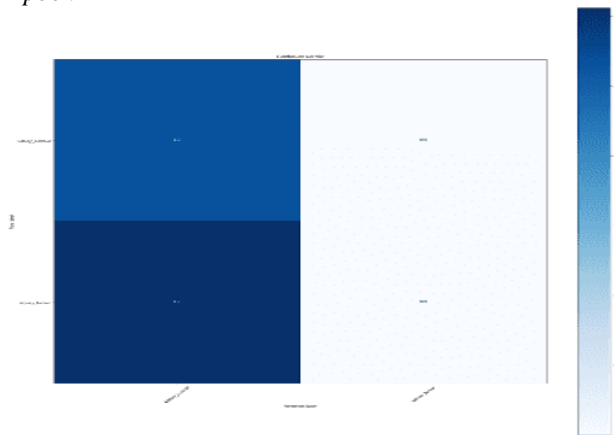


Figure 7: Confusion matrix at epoch =1

Accuracy=64% Loss= 0.20

**A. Epoch**

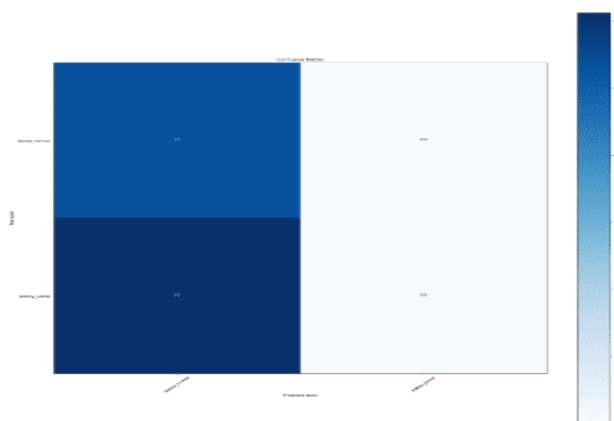


Figure 8: Confusion matrix at epoch =5

Accuracy =64%, Loss=0.22

*Epoch= 10*

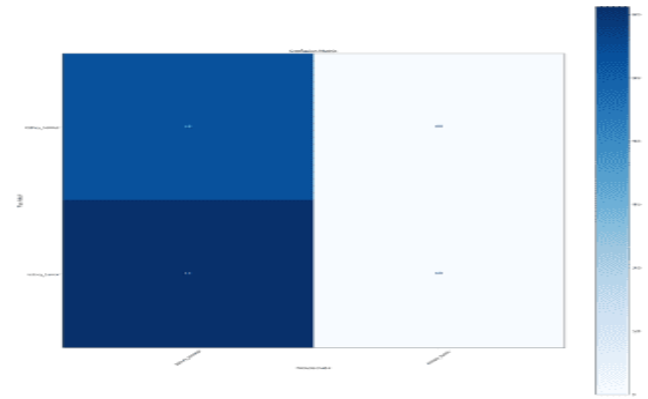


Figure 9: Confusion matrix at epoch =10

Accuracy = 69%, Loss= 0.69

Table 5: Results recorded in the model over a variety of epochs

Epoch	Accuracy	Loss
1	64	0.20
5	64	0.222
10	70	0.69

**V. CONCLUSION**

In the article, we describe a deep learning model for classifying the malignancy of kidney tumours. The purpose of this model is to act as a second opinion system, identifying malignant tumours that were misclassified in order to save needless procedures. We demonstrate that by enhancing the information transfer from pre-trained networks, medical picture colorization may raise the F1-score up to 1.8pp. We further demonstrate that adding more CT slices during training can enhance the network’s performance, increasing its F1score by up to 2.2 pp.

We demonstrate that such a system achieving high recall score is suitable for post-radiological diagnosis reevaluation, despite the fact that our research is limited by the fact that our solution is shown working in pair-with human diagnosis and additional research would need to be done to test it in a stand-alone fashion and compare it directly to radiological diagnosis.

We will continue to research medical picture colorization and its impact on image categorization in the future. Additionally, we intend to add segmentation pre-processing to the machine learning pipeline so that we may employ many CT slices in the prediction phase. This will allow us to accommodate majority-voting based approaches, which may help the network’s accuracy even more.

**CONFLICTS OF INTEREST**

The authors declare that they have no conflicts of interest.

**REFERENCES**

[1]. Aboutalib, S. S.; Mohamed, A. A.; Berg, W. A.; Zuley, M. L.; Sumkin, J. H.; and Wu, S. 2018. Deep learning to distinguish

- recalled but benign mammography images in breast cancer screening. *Clinical Cancer Research* 24(23):5902– 5909.
- [2]. Attique, M.; Gilanie, G.; Mehmood, M. S.; Naweed, M. S.; Ikram, M.; Kamran, J. A.; Vitkin, A.; et al. 2012. Colorization and automated segmentation of human t2 mr brain images for characterization of soft tissues. *PloS one* 7(3):e33616.
- [3]. Baghdadi, A.; Aldhaam, N. A.; Elsayed, A. S.; Hussein, A. A.; Cavuoto, L. A.; Kauffman, E.; and Guru, K. A. 2020. Automated differentiation of benign renal oncocytoma and chromophobe renal cell carcinoma on computed tomography using deep learning. *BJU Int* 125(4):553–60.
- [4]. Chollet, F. 2017. Xception: Deep learning with depthwise separable convolutions. In *Proceedings of the IEEE conference on computer vision and pattern recognition*, 1251– 1258.
- [5]. Cokkinides, V., A. J. S. A. e. a. 2020. American cancer society: Cancer facts and figures.
- [6]. Deng, J.; Dong, W.; Socher, R.; Li, L.-J.; Li, K.; and FeiFei, L. 2009. Imagenet: A large-scale hierarchical image database. In *2009 IEEE conference on computer vision and pattern recognition*, 248–255. Ieee.
- [7]. Erdim, C.; Yardimci, A. H.; Bektas, C. T.; Kocak, B.; Koca, S. B.; Demir, H.; and Kilickesmez, O. 2020. Prediction of benign and malignant solid renal masses: machine learningbased ct texture analysis. *Academic radiology* 27(10):1422– 1429.
- [8]. Han, S.; Hwang, S. I.; and Lee, H. J. 2019. The classification of renal cancer in 3-phase ct images using a deep learning method. *Journal of digital imaging* 32(4):638–643.
- [9]. He, K.; Zhang, X.; Ren, S.; and Sun, J. 2015. Deep residual learning for image recognition.
- [10]. Heller, N.; Sathianathen, N.; Kalapara, A.; Walczak, E.; Moore, K.; Kaluzniak, H.; Rosenberg, J.; Blake, P.; Rengel, Z.; Oestreich, M.; et al. 2019. The kits19 challenge data: 300 kidney tumor cases with clinical context, ct semantic segmentations, and surgical outcomes. *arXiv preprint arXiv:1904.00445*.
- [11]. Iandola, F.; Moskewicz, M.; Karayev, S.; Girshick, R.; Darrell, T.; and Keutzer, K. 2014. Densenet: Implementing efficient convnet descriptor pyramids. *arXiv preprint arXiv:1404.1869*.